DEVELOPMENT OF COLORIMETRIC SENSING ASSAY FOR CYSTEINE DETECTION USING ARDUINO BASED READ-OUT METHOD

M.Tech Thesis

By

Nandini Singh

DEPARTMENT OF BIOSCIENCES AND BIOMEDICAL ENGINEERING
INDIAN INSTITUTE OF TECHNOLOGY INDORE

May 2025

DEVELOPMENT OF COLORIMETRIC SENSING ASSAY FOR CYSTEINE DETECTION USING ARDUINO BASED READ-OUT METHOD

A THESIS

Submitted in partial fulfillment of the requirements for the award of the degree

of
Master of Technology

by

NANDINI SINGH

DEPARTMENT OF BIOSCIENCES AND BIOMEDICAL ENGINEERING
INDIAN INSTITUTE OF TECHNOLOGY INDORE
MAY 2025

INDIAN INSTITUTE OF TECHNOLOGY INDORE

CANDIDATE'S DECLARATION

I hereby certify that the work which is being presented in the thesis entitled **DEVELOPMENT OF COLORIMETRIC SENSING ASSAY FOR CYSTEINE DETECTION USING ARDUINO BASED READ-OUT METHOD** in the partial fulfillment of the requirements for the award of the degree of **MASTER OF TECHNOLOGY** and submitted in the **DEPARTMENT BIOSCIENCES AND BIOMEDICAL ENGINEERING , Indian Institute of Technology Indore**, is an authentic record of my own work carried out during the time period from July 2024 to May 2025 under the supervision of Dr. Abhijeet Joshi, Associate Professor, BSBE, IIT Indore.

The matter presented in this thesis has not been submitted by me for the award of any other degree of this or any other institute.

Nandini Singh 19/5/25

Signature of the student with date
(Nandini Singh)

This is to certify that the above statement made by the candidate is correct to the best of my/our knowledge.

AB Joshi 19/5/25

Signature of the Supervisor of
M.Tech thesis
(Dr. Abhijeet Joshi)

NANDINI SINGH has successfully given her M.Sc. Oral Examination held on **05 May 2025**

AB Joshi 19/5/25

Signature(s) of Supervisor(s) of M.Tech thesis
Date:

P.V. Kodgire

Convener, DPGC
Date: 19/05/2025

ACKNOWLEDGEMENTS

I would like to express my deepest gratitude to **Dr. Abhijeet Joshi**, my project instructor at the Department of Biosciences and Biomedical Engineering, IIT Indore, for his constant guidance, insightful feedback, and encouragement throughout this project.

I am also immensely thankful to my PhD seniors specially **Tileshwar Sahare, Badri Narayan Sahoo and Simran Rana** whose invaluable advice and support have played a crucial role in helping me overcome technical and conceptual challenges and my lab mates **Belal, Yashi, and Milan** for keeping the lab environment light and encouraging.

To my friends and batch mates, thank you for being a source of motivation, companionship, and light heartedness during stressful times. Your presence made this journey far more enjoyable and memorable.

A heartfelt thank you goes to my parents and family, whose unwavering love, belief in me, and emotional support formed the foundation upon which I was able to build this work. Your sacrifices and encouragement have made all the difference.

A very special thanks to **SLt Kushagra Deol**, whose unwavering support, patience, and encouragement have been my greatest strength throughout this journey.

Working on this project has been an incredibly enriching experience. I not only gained technical knowledge and hands-on skills in biosensing and embedded systems, but also learned the importance of patience, perseverance, and collaboration. I leave this phase with not just data and results, but with lessons, gratitude, and memories that will stay with me forever.

Dedicated to my family

Mr. Deep Kamal

Mrs. Vinita Singh

and Kushagra Deol

Abstract

This study presents the development of a simple, rapid, and highly selective colorimetric detection method for cysteine based on its interaction with a Chromium (III) chloride hexahydrate and diphenylcarbazone (DPC) complex. The sensing mechanism relies on the ability of cysteine to reduce the Cr-DPC complex, leading to a distinct color change from purple to green. This reaction completes within 30 minutes and is easily visible to the naked eye, allowing preliminary detection without sophisticated instrumentation. Cysteine detection is clinically significant due to its relation to cystinuria, a rare inherited disorder characterized by defective renal reabsorption of cystine and other dibasic amino acids. Excess cystine in the urine leads to the formation of cystine stones, causing recurrent kidney stone episodes, pain, and potential kidney damage. Monitoring cysteine or cystine levels in urine is essential for early diagnosis and effective disease management in cystinuria patients. Interference studies using physiologically relevant urinary analytes (urea, creatinine, amino acids, ions, glucose, etc.) demonstrated no significant interference, confirming the system's high selectivity toward cysteine. pH studies further validated the sensor's stability under varying urine-like conditions. The colorimetric response gradually intensified up to 9 hours due to complex stabilization but diminished slightly at 24 hours, likely due to environmental degradation. As a future perspective, a portable Arduino Mega 2560-based analytical device is proposed, integrated with a TCS230 color sensor programmed to convert RGB data to HSV values for higher accuracy.. Such a system would be highly beneficial for cystinuria patients, enabling routine monitoring of cysteine levels to prevent stone formation, improve treatment outcomes, and reduce hospital visits

LIST OF PUBLICATIONS

Sahare, T., Singh, N., Sahoo, B. N., & Joshi, A. (2024). Smartphone-enhanced nanozyme sensors. Colorimetric and fluorescence sensing techniques. *Biosensors and Bioelectronics. X*, 100544.

TABLE OF CONTENTS

LIST OF FIGURES

Chapter 1

Introduction

Accurate and accessible methods for detecting biomolecules are critical for advancements in clinical diagnostics, environmental monitoring, and quality control. Here, we have presents the development of a colorimetric assay for the detection of cysteine, utilizing the unique chemical interaction between chromium chloride, diphenylcarbazide (DPC), and cysteine[1]. This complex exhibits characteristic chromogenic properties, which are further modulated upon interaction with cysteine. Cysteine reacts with the Cr-DPC complex, leading to a shift in the color gradient from reddish-purple to green colour , with the RGB green intensity directly correlating to cysteine concentration[2]. The assay's visual response was analyzed using RGB (Red-Green-Blue) image processing, focusing on the green channel intensity to quantify cysteine levels. The chemical reactions and the resulting chromogenic shifts were systematically studied to establish a reproducible trend. The RGB data will be further processed in MATLAB to create a calibration model mapping RGB intensity to precise concentrations[3].Future goals will include the use of AI models such as XGBoost[4] and Scikit-learn[5], to improve the reliability of image analysis by addressing variations in lighting and sample conditions. Moreover, efforts are underway to integrate this assay into a portable detection system using Arduino-based technology, paired with a mobile application for real-time image capture and data processing[6]. This comprehensive approach combines chemical analysis, computational modelling, and engineering design to create a robust, user-friendly platform for cysteine quantification. The proposed system is expected to bridge the gap between laboratory-based methods and field-ready diagnostic tools, offering significant potential for applications in resource-limited settings. The most frequent genetic cause of paediatric nephrolithiasis is cystinuria. Since the genetic abnormality affects the reabsorption of cystine and three other amino acids (arginine, lysine, and

ornithine) in the renal proximal tubule, it is regarded as a heritable aminoaciduria[7]. Because cystine is an amino acid that is poorly soluble at normal urine pH, patients with this illness have higher excretions of cystine in their urine, which can lead to the formation of cystine calculi. SLC3A1 and SLC7A9, which encode the two subunits of the heterodimeric transporter, are the two genes that have been identified as disease-causing thus far [7] . This condition's clinical manifestations are only associated with nephrolithiasis. Although late diagnosis is frequent, the diagnosis is typically made in infancy or adolescence. Of the 41 individuals with a positive Brand test, 39 (1.9%) had pathological cystinuria confirmed. While the age of stone beginning was 21.8 +/- 12.4, the mean age of cystine stone patients was 38.1 +/- 15.8 years. Six patients were seen at the onset of renal stones, whereas 85% of cases had recurrent stones. The ratio of men to women was 1.0.62. The patient experienced 18.5 +/- 35.8 stone bouts on average, with 4.1 +/- 4.3 years between the first recurrence. Five years following the initial kidney stone, 83% of cases recurred. In addition, we looked at 85 individuals of 24 families whose relatives had cystine stones. Only five (21%) of the twenty-four family members who had high cystine excretion had cystine calculi [8].

The development of sensitive and cost-effective methods for detecting and quantifying biomolecules is a critical need in analytical chemistry and biosciences. Colorimetric assays, which rely on visually detectable or spectrophotometrically measurable color changes, have gained prominence due to their simplicity, reliability, and potential for point-of-care applications. Among various chemical systems used in colorimetric detection, the interaction between $CrCl_3$ and DPC can emerged as a versatile tool, owing to its ability to form a distinct, chromogenic complex.

DPC is know for its ability to form a stable, colored complex with chromium ions, particularly Cr(VI) and Cr(III). This complex exhibits unique spectral properties, making it an ideal candidate for use in quantitative analysis[9]. In

this study, we explored how this Cr-DPC complex interacts with varying concentrations of cysteine, an essential amino acid with significant biological and industrial importance. The interaction results in noticeable shifts in the color intensity of the solution, creating a color gradient that can be quantified for analytical purposes[10]. Cysteine accurate measurement is essential in various fields, including clinical diagnostics, pharmaceutical quality control, and environmental monitoring. Leveraging the reactivity of cysteine with the Cr-DPC complex, we developed a straightforward and efficient colorimetric assay to determine cysteine concentrations.

A key advantage of the developed Cr-DPC-cysteine assay lies in its ability to produce a visually distinguishable green color gradient that corresponds to different cysteine concentrations. This shift in color intensity, which arises from the interaction between cysteine and the Cr-DPC complex, provides a basis for accurate quantification. To enhance the precision of the analysis, the RGB (Red-Green-Blue) color model[11–13] was employed to capture and analyse the colour variations across the concentration range.

Using RGB analysis, the green channel intensities of the assay solutions were extracted and correlated with cysteine concentrations. Images of the solutions were captured under consistent lighting conditions using a standard phone camera, ensuring accuracy. The green intensity values were then processed using Color Grab[14,15]application, this enabled the development of a calibration curve that directly linked the green channel intensities in a way that when concentration of cysteine increases the corresponding green channel intensity was increasing, to the corresponding cysteine concentrations. This analysis approach not only minimized human error but also allowed for precise and reproducible data interpretation.

Chapter 2

Review of Past Work and Problem Formulation

Cystine is amino acid, composed of dual cysteine molecules bonded via a disulfide bond. In this disease faulty trans-epithelial transporters of the dibasic amino acids, ornithine, cystine, arginine, lysine, and ("COLA amino acids") within each the renal proximal tubules and the intestinal tract. But due to its low solubility at physiological urinary pH, over-excretion of cystine in the kidney ends in the remarkable-saturation of cystine inside the urine and formation of cystine crystals and sooner or later stones. Stone formation in cystinuria is due to free solution crystallization[16]. Cystinuria is an autosomal recessive disease[17]; however, some heterozygote carriers have an autosomal dominant, incomplete penetrance appearance with elevated, but typically non-pathological urinary cystine excretion, but because of this abnormality, prior,to genetic analysis cystinuria sufferers havebeen phenot ypically classified as both type I or non-type I (type II or type III) based on urinary excretion and GI absorption[18] of cystine within the parents (obligate heterozygotes) of sufferers Non-type I carrier can present with symptomatic cystine stones, even though not often. The physiology of cystine absorption is concept to include precise amino acid transporters inside the kidney and GI tract Cystine and the dibasic amino acids are absorbed from the urinary lumen into the proximal tubules through covalently linked heterodimer amino-acid transporters—rBAT and B(0,+) AT—found on the luminal face of each the GI tract and the proximal tubules of the kidney[19].

Excessive urinary cystine levels are indicative of cystinuria[20], that's characterised through impaired reabsorption of cystine in the kidneys. This circumstance can lead to recurrent kidney stones, often presenting symptoms which includes flank pain, hematuria, and urinary tract infections[21]. Monitoring cystine levels helps prevent complications related to kidney stones, which include urinary obstruction, chronic kidney

disorder, and acute renal failure due to stone-associated blockages. Early detection permits for timely interventions, which include improved fluid intake and dietary adjustments[22]. As the cystinuria results in urinary growth in L-cystine stage and growth of cystine stones[23], L-cystine is for that reason the maximum considerable biomarker for the accurate and early analysis of cystinuria[24]. Therefore, keeping their levels in check is vital for early prevention, analysis and treatment. [25] The purpose of the project is to design a sensitive and practical colorimetric assay for detecting cysteine concentrations by utilizing the interaction between cysteine and a Cr-DPC complex. This assay will produce a visually distinct color gradient that correlates with cysteine levels. The assay's readout will rely on RGB analysis, where images of the reaction mixtures are captured using a standard camera under uniform lighting conditions. The green channel intensity from these images is extracted and analyzed to establish a quantifiable trend corresponding to cysteine concentration. To refine the accuracy of this method, MATLAB will be used to model the colorimetric responses and generate calibration curve. This curve will serve as the baseline for mapping the RGB intensities to specific cysteine concentrations. In the long term, this research aims to translate the laboratory-based assay into a portable and user-friendly device. By integrating the assay with an Arduino-based detection system, a device will be developed to capture, process, and analyze images directly. The integration of a mobile application will further simplify the workflow, allowing users to obtain real-time cysteine concentration readings.

Contemporary Diagnostic Approaches for Cystinuria Detection

The detection of cystinuria has evolved significantly in recent years, incorporating both established techniques and innovative methodologies that enhance diagnostic precision, safety, and clinical applicability. These methods are employed for both preliminary screening and confirmatory

diagnosis, with advancements improving sensitivity, specificity, and overall reliability.

1. Urinalysis and Microscopic Crystal Identification

Routine urine examination remains an essential diagnostic tool. Microscopic evaluation of urinary sediment frequently reveals hexagonal, flat cystine crystals—hallmarks of cystinuria—which are observed in a substantial proportion of untreated individuals. These crystals are considered pathognomonic for the disease. Additionally, urinalysis may reveal a characteristic sulfurous odor, often described as reminiscent of rotten eggs, due to the sulfur-rich nature of cystine.[26]

2. Preliminary Qualitative Tests

One of the earliest screening methods for cystinuria is the sodium nitroprusside test, which induces a purple coloration upon reacting with elevated concentrations of cystine in urine. Although it allows for rapid detection, the test is prone to false-positive results and has limited sensitivity, reducing its diagnostic utility. Consequently, it is now regarded as obsolete for routine clinical use. To enhance test safety and reliability, recent modifications involve the use of borohydride as a reducing agent instead of cyanide, improving the method's feasibility in clinical settings.

3. Quantitative Assessment of Urinary Cystine

The quantification of cystine excretion over a 24-hour period remains the cornerstone of cystinuria diagnosis. Analytical techniques such as ion-exchange chromatography and liquid chromatography coupled with tandem mass spectrometry (LC-MS/MS) are employed to accurately measure cystine levels, along with associated dibasic amino acids including ornithine, lysine, and arginine. In recent developments, amperometric detection methods using silver electrodes have emerged as cost-effective and straightforward alternatives. These electrochemical approaches allow

for direct cystine measurement and hold promise for point-of-care applications.

4. Assessment of Cystine Solubility and Supersaturation

The cystine capacity test evaluates the extent to which a patient's urine can solubilize an added quantity of solid cystine. This test provides a functional assessment of cystine saturation and is especially relevant in patients undergoing treatment with thiol-based agents, where conventional supersaturation testing may not yield reliable results. Despite being technically demanding, the test offers high diagnostic value. Alternatively, cystine supersaturation can be directly calculated using software models based on urinary composition, which assists in evaluating stone formation risk and tailoring therapeutic strategies.

5. Analysis of Stone Composition

The definitive characterization of urinary calculi, especially to confirm cystine content, is achieved using techniques such as Fourier-transform infrared (FTIR) spectroscopy and X-ray diffraction. These methods provide precise molecular and crystalline analysis, essential for the accurate classification of stone types and guiding appropriate management.

6. Radiological Detection of Cystine Stones

Imaging plays a critical role in identifying cystine urolithiasis. Non-contrast computed tomography (CT) is considered the most sensitive and specific modality for stone detection[27]. Cystine calculi typically exhibit low radiodensity, generally less than 800 Hounsfield units, rendering them faintly radio-opaque. While CT is the gold standard, ultrasonography is often preferred in pediatric populations and during pregnancy due to its non-ionizing nature. It can detect larger calculi and complications such as hydronephrosis. Plain abdominal radiography (KUB) is less sensitive, as cystine stones are only mildly radiopaque and may be overlooked on standard X-rays.

7. Molecular Genetic Testing

Genetic confirmation of cystinuria involves identifying mutations in the *SLC3A1* and *SLC7A9* genes, which encode subunits of the amino acid transporter responsible for cystine reabsorption in the renal tubules. Next-generation sequencing (NGS) platforms are increasingly utilized for this purpose, offering comprehensive analysis capable of detecting both point mutations and larger genomic alterations. NGS surpasses traditional Sanger sequencing in scope and resolution. Additionally, multiplex ligation-dependent probe amplification (MLPA) and real-time polymerase chain reaction (PCR) techniques are employed to identify large-scale deletions or duplications within the target genes, further enhancing diagnostic accuracy.[28]

Chapter 3

Experimental

- **Reagents**

All reagents used were analytical grade. Chromium chloride hexahydrate ($CrCl_3.6H_2O$), 1,5-Diphenylcarbazone ($C_{13}H_{12}N_4O$), L-Cystine ($C_6H_{12}N_2O_4S_2$), were purchased from SRL. All glassware and magnetic stirrer bars were cleaned using freshly prepared aqua regia (HCl/HNO_3, 3.1), followed by thorough rinsing with ultrapure water and air drying.

- **Instrument**

UV–vis spectra were obtained using a UV–vis Spectrophotometer (SHIMADZU UV–vis 2600 PC, Japan) with baseline correction in the range of 200–800 nm. Fourier Transform Infrared (FTIR) spectra were recorded on a Thermo Scientific Nicolet iS10 (USA) in Attenuated Total Reflectance (ATR) mode, with baseline correction applied over the wavenumber range of 4000–400 cm^{-1}.

For the detection of different concentration of cysteine, complex is prepared by adding chromium chloride and diphenyl carbazide in optimum ratios.

3.1. Preparation of DPC Solution

The DPC solution was prepared by dissolving **2 mg of DPC** in **1 mL of 99% ethanol** to achieve a concentration of **2 mg/mL**. This corresponds to a molar concentration of approximately **8.26 mM**, calculated based on the molecular weight of DPC. The solution was mixed thoroughly to ensure complete dissolution of the DPC in ethanol, and care was taken to avoid exposure to light, as DPC is light-sensitive. The prepared DPC solution was stored in a foil wraped container at room temperature.

3.2. Preparation of Chromium Chloride Solution

A stock solution of **1 M chromium chloride ($CrCl_3$)** was prepared by dissolving the required amount of chromium chloride in deionized (DI) water at room temperature. For the assay, the stock solution prepared was of **1 mM concentration** by mixing 10 mL of DI water with 1.33gm of chromium chloride. The solution was mixed thoroughly to ensure homogeneity. The diluted solution was stored at room temperature in a sealed container to minimize contamination or evaporation.

3.3. Preparation of Cysteine Stock Solution

A **1 mM stock solution** of cysteine was prepared by first dissolving the 121mg of cysteine in **1N HCl**. The acid was used to make cysteine soluble in the solution. Once the cysteine was fully dissolved, the solution was diluted to a final volume of **10 mL** using **citrate buffer**. The citrate buffer was specifically chosen to maintain the pH of the solution within the range of **6 to 6.4**, which is ideal pH of urine. The final cysteine solution, at a concentration of **1 mM**, was stored at 4°C and used for preparing a range of cysteine concentrations for the assay.

Chapter 4

Results and discussion

4.1. U V-Visible spectra and FTIR (Fourier Transform Infrared spectroscopy) spectra of Compounds

UV-Vis spectroscopic analysis was performed to evaluate the absorption profiles of $CrCl_3$, DPC, cysteine, and the resulting Cr-DPC-cysteine complex. The individual compounds exhibited distinct absorption peaks.

4.1.1 DPC

Diphenyl carbazone is an organic dye (Fig. 4). It contains two phenyl rings form the backbone, providing hydrophobic and π-conjugated properties and a chain with alternating nitrogen (N) and oxygen (O) atoms, including a hydrazone (-NH-N=) group. The carbazone group is responsible for metal ion chelation and color changes due to electron delocalization (Fig. 1).

The system's conjugated structure facilitates absorption of visible light, making it a chromophore. This property gives the dye its ability to change color in the presence o4f specific ions, depending on the pH and other chemical environments.

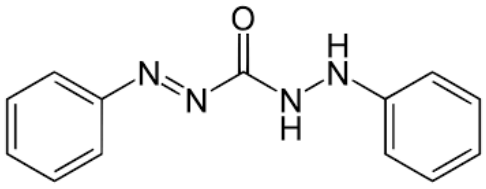

Fig. 1. Structure of DPC

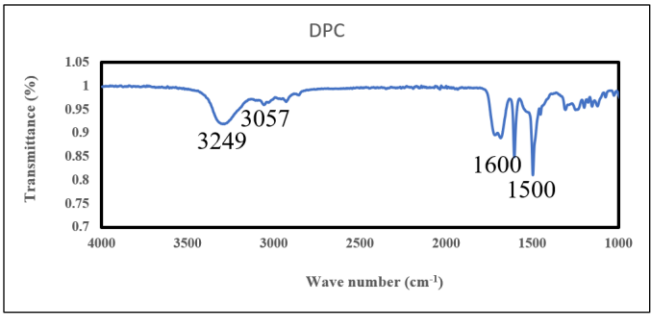

Fig. 2. FTIR of DPC

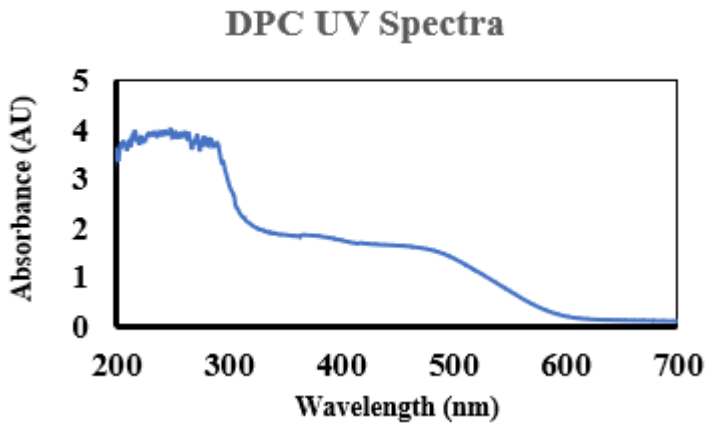

Fig. 3. UV-vis absorption spectrum of DPC

- The FTIR spectral analysis of DPC reveals significant peaks that provide insights into its functional groups and chemical structure (Fig. 2). A prominent peak at 3249 cm^{-1} corresponds to N-H stretching vibrations, characteristic of the aliphatic primary amine group present in the molecule. This confirms the presence of the hydrazine moiety, a key reactive site in DPC. Additionally, strong peaks observed at 1600 cm^{-1} and 1500 cm^{-1} are attributed to C=O stretching vibrations and the aromatic ring structure, respectively. These peaks indicate the presence of carbonyl groups and the aromatic framework that contribute to the chromogenic properties of DPC.

Fig. 4. Image of DPC dissolved in 99% ethanol

4.1.2 $CrCl_3$

Chromium chloride is an inorganic compound. It exists in multiple oxidation states, with $CrCl_3$ being the most stable form (Fig. 5). $CrCl_3$ is typically found as a dark green crystalline solid that is highly soluble in water, forming a hydrated complex. The compound's ability to form stable coordination complexes with various ligands makes it a versatile reagent.

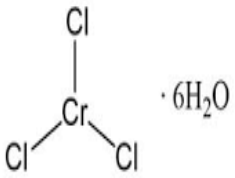

Fig. 5. Structure of $CrCl_3.6H_2O$

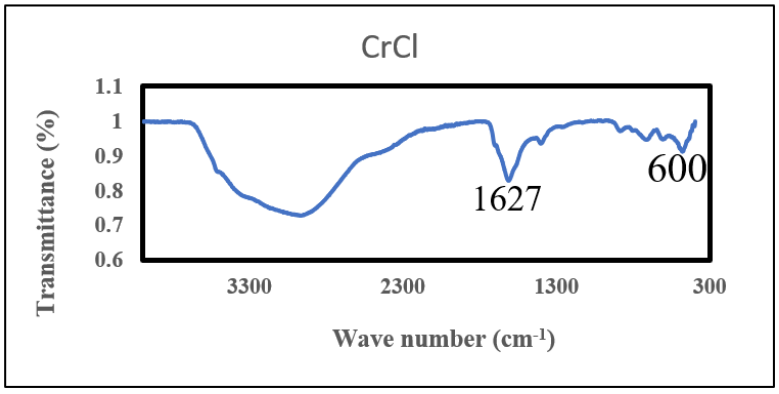

Fig. 6. Chromium chloride FTIR Spectra

- The FTIR spectral analysis of $CrCl_3$ provides valuable insights into its molecular structure and bonding. Peaks observed below 600 cm^{-1} are characteristic of metal-halide interactions, specifically attributed to the stretching vibrations of the Cr-Cl bonds. These peaks confirm the strong coordination between chromium and chlorine atoms in the compound. Additionally, a distinct peak near 1627 cm^{-1} corresponds to H-O-H bending vibrations, indicating the presence of water molecules, likely from hydration or moisture in the sample (Fig. 6).

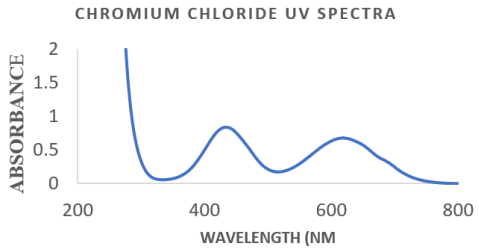

Fig. 7. Chromium chloride UV Spectra

- The UV-Vis spectral analysis of chromium chloride ($CrCl_3$) revealed absorption peaks at 436 nm and 621 nm, closely aligning with the reported values of 432 nm and 621 nm. These peaks are characteristic of d-d electronic transitions in the Cr^{3+} ion, reflecting its octahedral ligand field environment. The slight shift in the 436 nm peak compared to the reported value may be attributed to variations in solvent, concentration, or sample conditions during the analysis. This consistency confirms the expected electronic behavior of $CrCl_3$ in solution (Fig. 7).

4.1.3 Complex of DPC and $CrCl_3$

When $CrCl_3$ is mixed with DPC in an aqueous solution, the Cr^{3+} ion displaces some or all of its chloride ligands to coordinate with the electron-donating sites on DPC. Typically, the oxygen atom from the carbonyl group

and one of the nitrogen atoms from the hydrazine group coordinate with the chromium centre, forming a chelate ring. This bidentate coordination stabilizes the complex. The complex formed gives dark purple colour (Fig. 10)

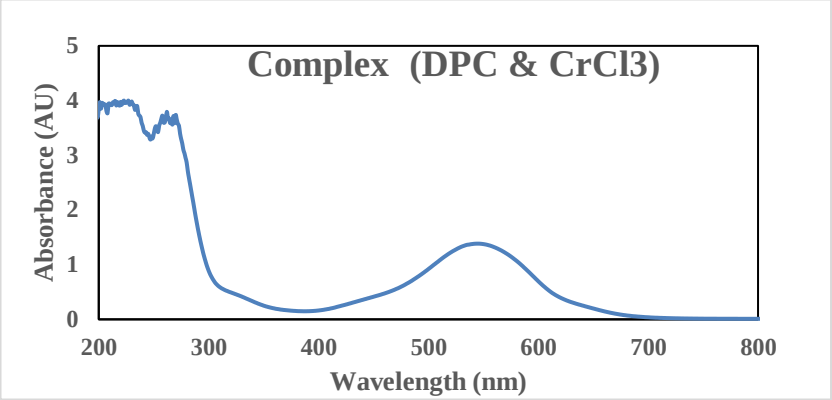

Fig. 8. UV Spectra of complex

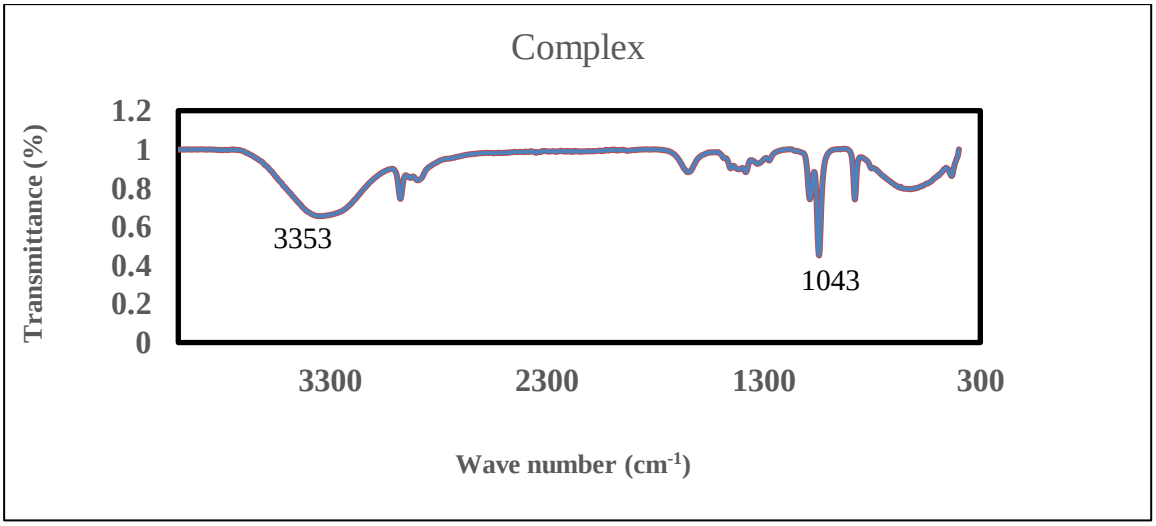

Fig. 9. FTIR Spectra of complex

Fig. 10. Image of complex

4.2. Selection of complex ratio

- Two complexes were analysed with UV-Visible spectroscopy (Fig. 8).
  - **3.1 Complex**. This means the ratio of DPC to $CrCl_3$ is 3.1.
  - **6.1 Complex**. This means the ratio of DPC to $CrCl_3$ is 6.1.
- The UV spectra were recorded at different time intervals. 30 minutes, 1 hour, 8 hours, and 12 hours.

Observation. -Both graphs show absorbance values across a range of wavelengths (200–800 nm). A peak around **542 nm** is significant for indicating the formation of the complex. Over time, the intensity of the peak changes, suggesting the progress or stability of the complex formation (Fig. 11).

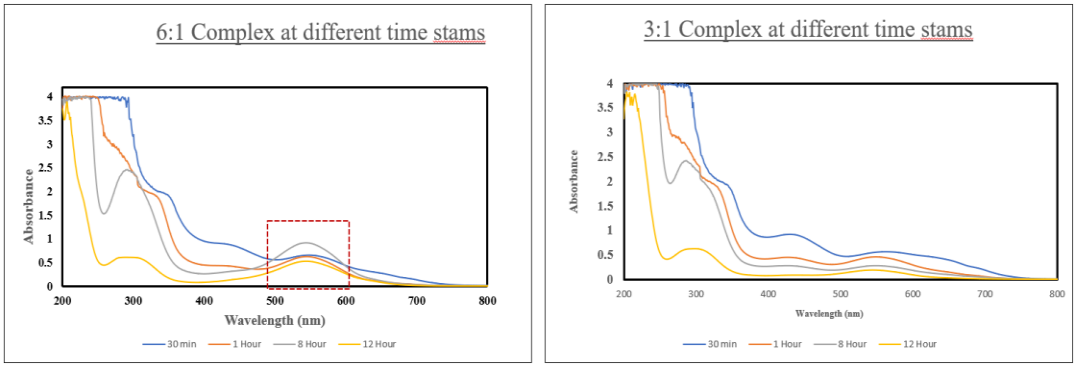

Fig. 11. - Time dependent study of different complex ratio

4.3. Interaction of Complex with cysteine concentrations

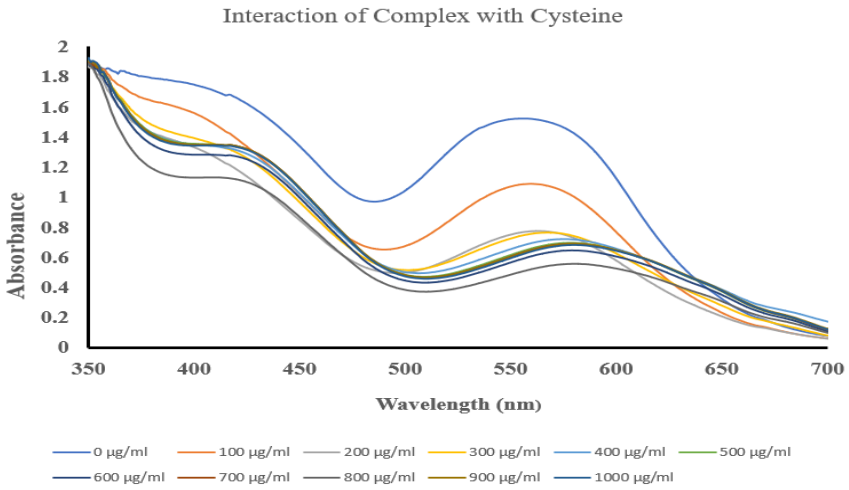

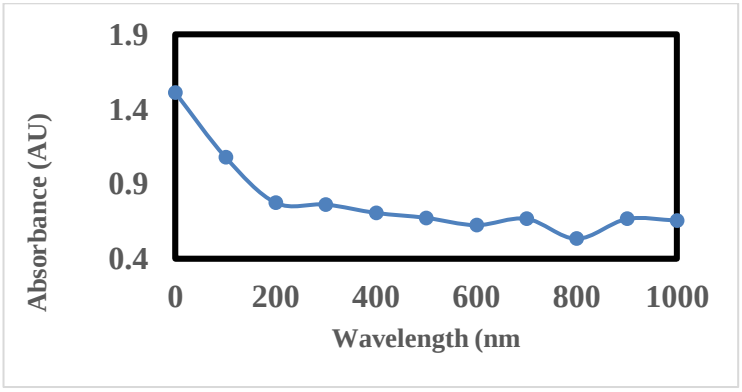

Fig. 12. UV Spectra of interaction of cysteine and complex

The diminishing absorbance suggests that the chromophore environment of the complex is being altered, likely due to direct interaction with cysteine. The spectral shift in the second graph indicates that the thiol group of cysteine is coordinating with a component of the complex, resulting in changes to the electronic environment. The interaction appears to cause a

visible color change, which is consistent with modifications in the complex's electronic transitions caused by binding of cysteine.

The binding is likely to occur through the thiol group of cysteine attaching to the metal centre in the complex (possibly Cr in the $CrCl_3$-DPC complex), as thiols have high affinity for metals. This interaction forms a new coordination structure, leading to the observed spectral changes. The color gradient reinforces the idea that the binding is concentration-dependent, providing further support for the interaction hypothesis. The colour gradient is shown below in Fig. 15. (A)

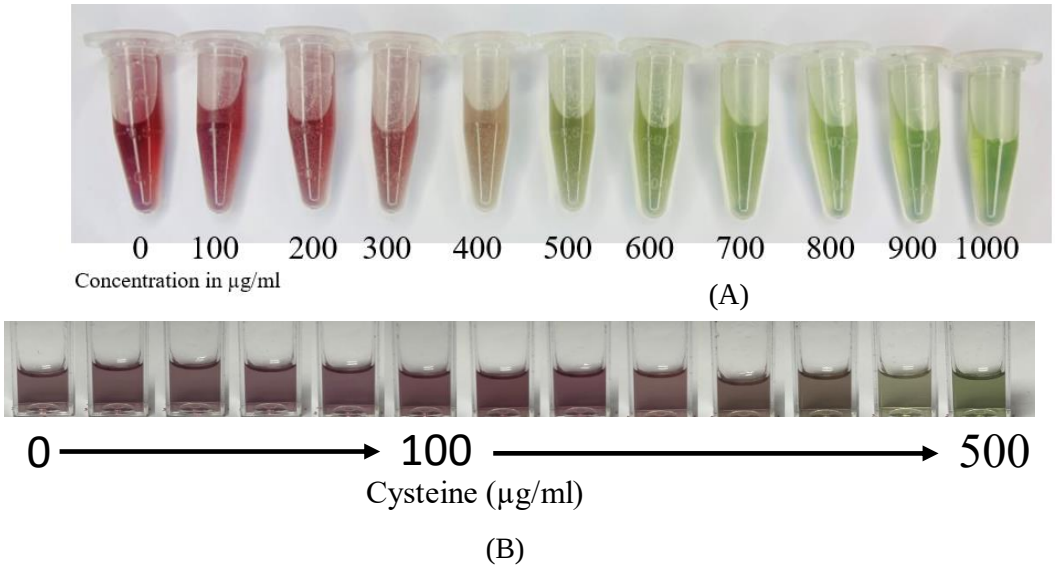

Fig. 13. Visible colour gradient (A) in higher ranges and (B) lower ranges

- **FTIR Analysis of interaction**

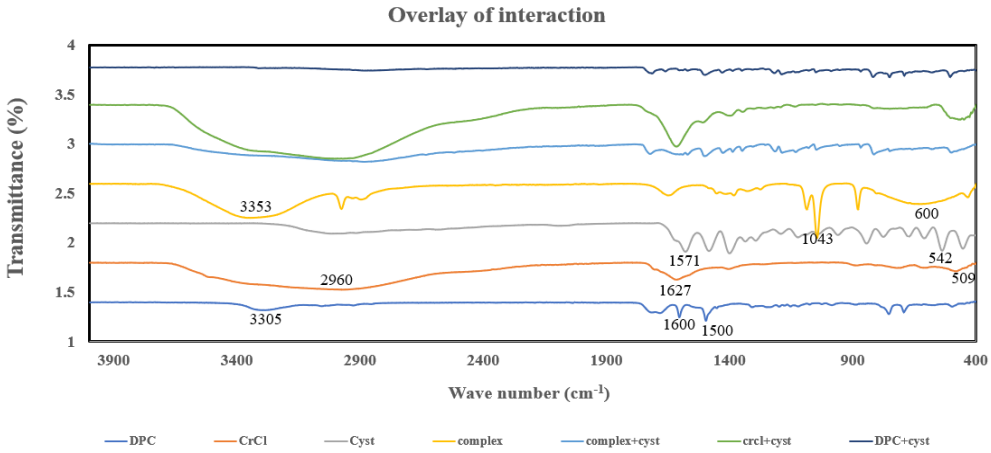

(A)

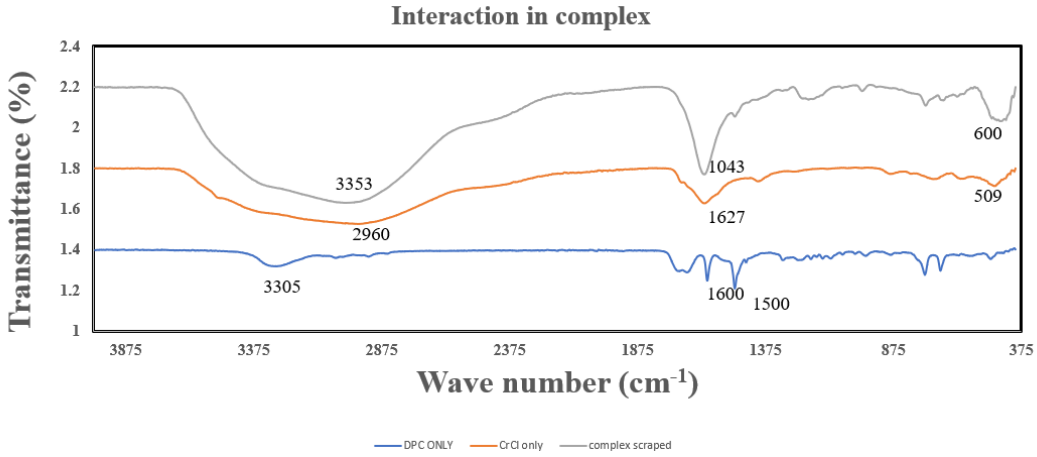

(B)

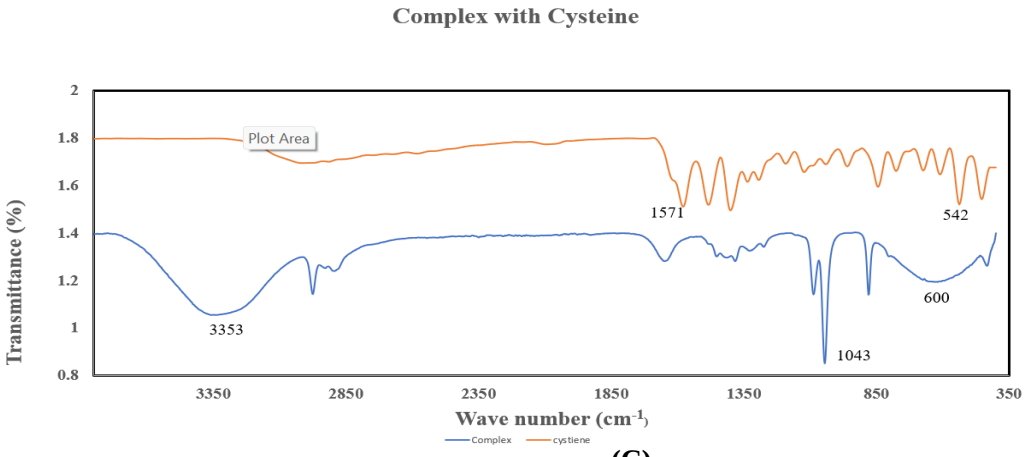

(C)

Fig. 14. -FTIR spectra of (A)-Overlay of interaction

(B)-Complex, $CrCl_3$, DPC

(C)-Complex and Cysteine

- In these overlay graphs of interaction, the peak at 1043 cm^{-1} indicates C-O or C-N bond vibrations, suggesting ligand coordination to the metal center. Peaks in the 500–700 cm^{-1} range correspond to metal-oxygen or metal-nitrogen stretching, confirming complex formation. The shift and reduction in intensities of the characteristic peaks suggest interaction between the thiol (-SH) group of cysteine and the complex, likely involving coordination with the metal center, leading to structural rearrangements. These observations confirm the formation of the complex and its interaction with cysteine through thiol binding, supported by significant spectral shifts (Fig. 14).

4.4.RGB Analysis

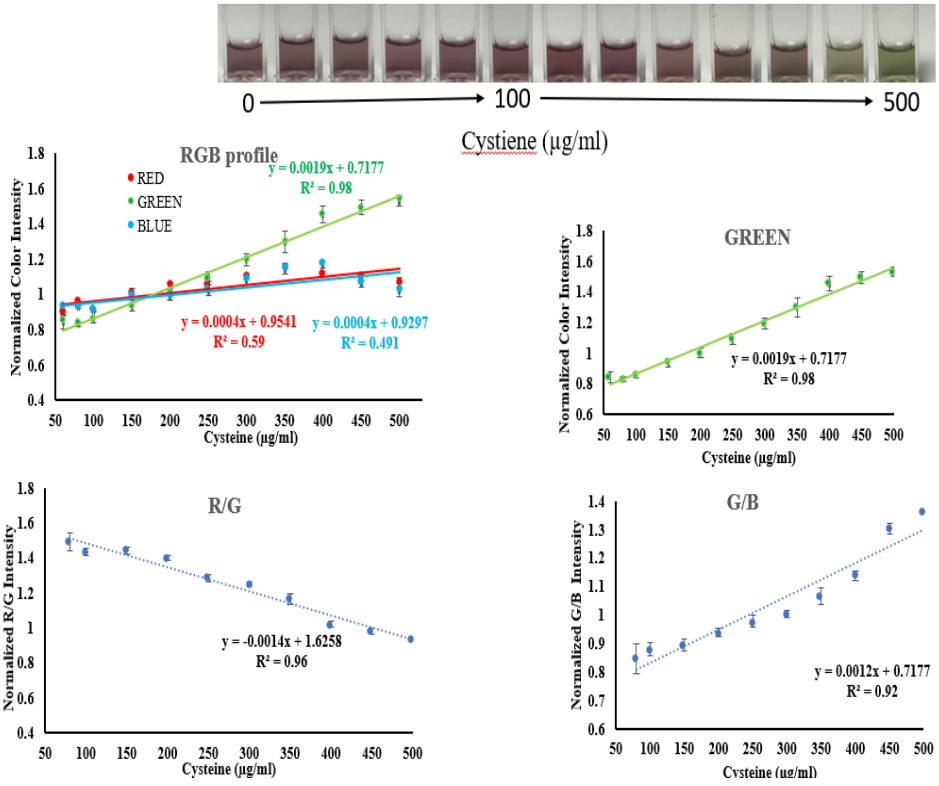

Fig. 15. -RGB profile graphs

	LOD (µg/ml)	LOQ(µg/ml)	% RSD	R^2
GREEN	7.6	23	2.7	0.98
R/G	9.5	28	5.9	0.96
G/B	7.8	23	8.3	0.92

Fig. 16. -RGB Analysis and LOD, LOQ, %RSD and R^2

The intensity of the green channel increases with the interaction of cysteine and the complex, indicating a shift in the visible spectrum's green region.

- **R^2 Value = 0.98**, indicates a very strong correlation between cysteine concentration and the green channel intensity.
- **LOD (Limit of Detection) = 7.6 µg/mL**. The minimum cysteine concentration detectable using this green channel intensity.
- **LOQ (Limit of Quantitation) = 23 µg/mL**. The minimum cysteine concentration quantifiable.

%RSD (Relative Standard Deviation) = 2.7%. The low %RSD suggests excellent precision for this parameter (Fig. 16).

➢ **R/G Ratio**.

- The red-to-green (R/G) intensity ratio decreases as cysteine concentration increases. This implies that the red intensity is reducing relative to the green intensity, confirming the color shift.
- **R^2 Value = 0.96**. A strong correlation between R/G ratio and cysteine concentration.
- **LOD = 9.5 µg/mL**, **LOQ = 28 µg/mL**, **%RSD = 5.9%**. These values indicate slightly reduced sensitivity and precision compared to the green channel alone.

➢ **G/R Ratio**.

- The green-to-red (G/R) intensity ratio increases with increasing cysteine concentration, reinforcing the observation of enhanced green channel intensity relative to red.
- **R^2 Value = 0.92**. Still a strong correlation, though slightly lower than the green channel or R/G ratio.
- **LOD = 7.8 µg/mL**, **LOQ = 23 µg/mL**, **%RSD = 8.3%**. These values show good sensitivity but slightly lower precision for this parameter.

The results from UV-Vis spectroscopy, FTIR analysis, and RGB colorimetric evaluation collectively confirm the interaction of the complex with cysteine, primarily through the thiol (-SH) group of cysteine.

- **UV-Vis Spectroscopy**.

  The UV-Vis analysis demonstrates a clear concentration-dependent interaction between the complex and cysteine. The significant decrease in absorbance at the characteristic peak around 542 nm indicates structural alterations in the complex due to cysteine binding.

  Cysteine's thiol group with the metal in the complex interaction disrupts the chromophoric system, leading to changes in the optical properties of the complex and the resulting color gradient.

- **FTIR**

  FTIR analysis supports the structural characterization of the complex and confirms the interaction with cysteine. The complex exhibited characteristic peaks at 500–700 cm^{-1}, confirming metal-oxygen or metal-nitrogen coordination, and at 1043 cm^{-1}, indicating metal-ligand interactions. Upon interaction with cysteine, notable shifts in these peaks were observed, suggesting the binding of cysteine to the metal center, likely through the thiol group.

  Additionally, the absence or reduction of characteristic thiol vibrations from cysteine in the combined spectra indicates thiol-metal coordination.

4.5.Urine spike study

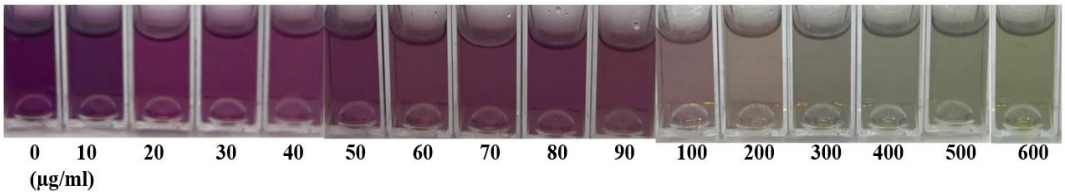

(a)

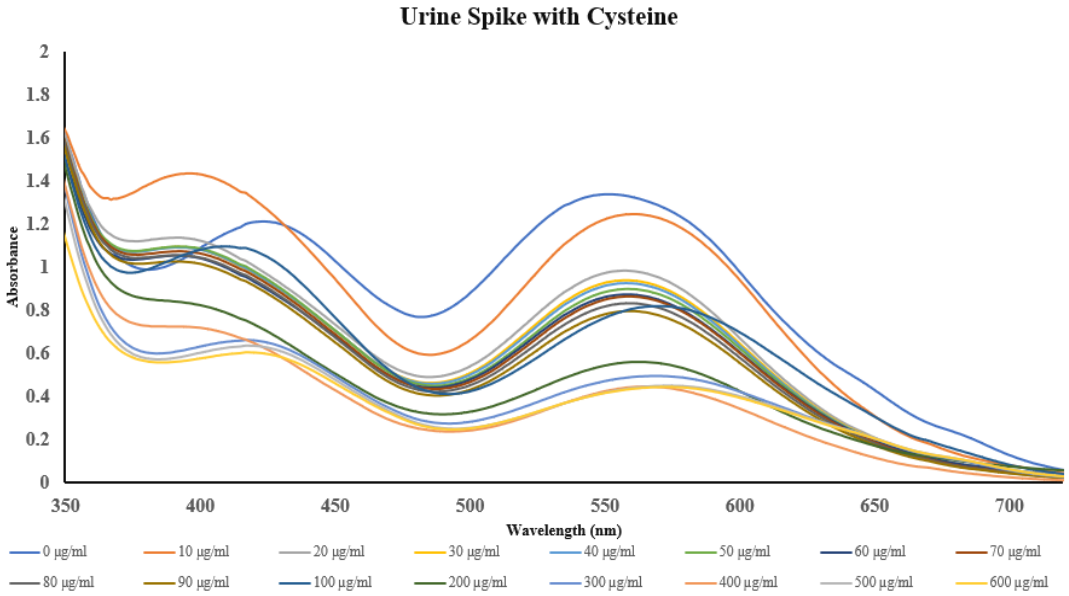

(b)

Fig. 17. - Urine spike study

(a) Colour gradient obtained

(b) UV-Vis Spectrum

The analysis of cysteine in urine samples spiked with varying concentrations of cysteine (0–600 µg/mL) using the complex of chromium chloride (CrCl) and diphenylcarbazone. In panel (A), a distinct color gradient is observed, transitioning from deep purple at lower concentrations to pale green at higher cysteine levels, indicating the disruption of the CrCl-diphenylcarbazone complex by cysteine. Panel (B) presents the UV-visible spectra of the spiked urine samples, showing absorbance patterns across

350–700 nm wavelengths. The spectra reveal a decrease in absorbance intensity as cysteine concentration increases, particularly around 500 nm, which corresponds to the characteristic peak of the intact complex. This reduction in absorbance suggests a competitive interaction or reduction effect caused by the thiol group in cysteine, leading to decolorization. The calibration curve derived from these data highlights the method's potential for quantifying cysteine concentrations in biological samples with high sensitivity and precision. The LOD, LOQ, %RSD and R2 of RGB analysis obtained is given in Fig. 18.

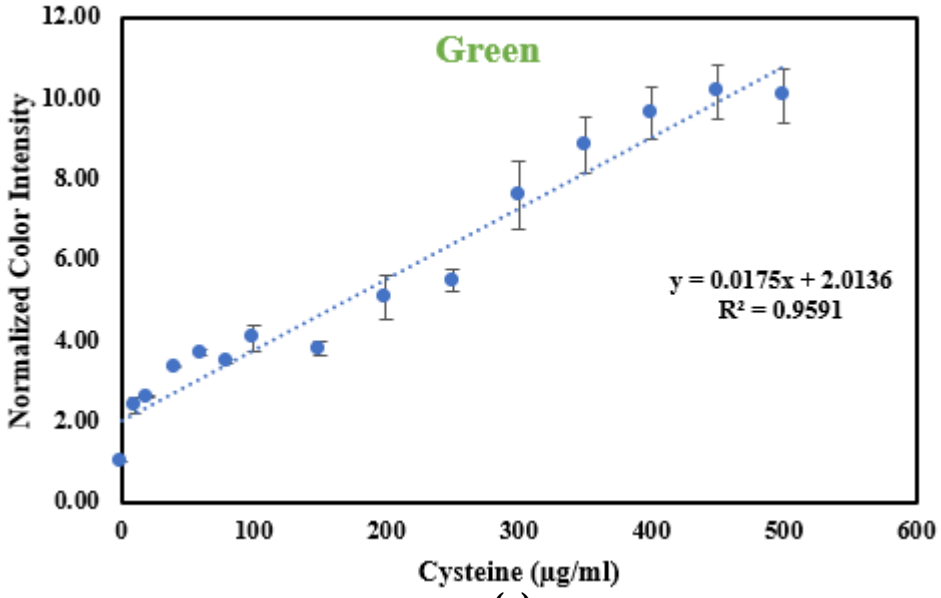

(a)

	LOD (µg/ml) Buffer	LOD (µg/ml) Urine	LOQ(µg/ml) Buffer	LOQ(µg/ml) Urine	% RSD Buffer	R^2 Buffer	R^2 Urine
Green	7.6	14.8	23	45	2.7	0.98	95
R/G	9.5	7	28	22.2	5.9	0.96	94
G/B	7.8	22	23	68.4	8.3	0.92	93

(b)

Fig. 18. RGB analysis

(a) Green channel intensity
(b) Comparative LOD, LOQ, %RSD and R^2

4.6.Interference Study

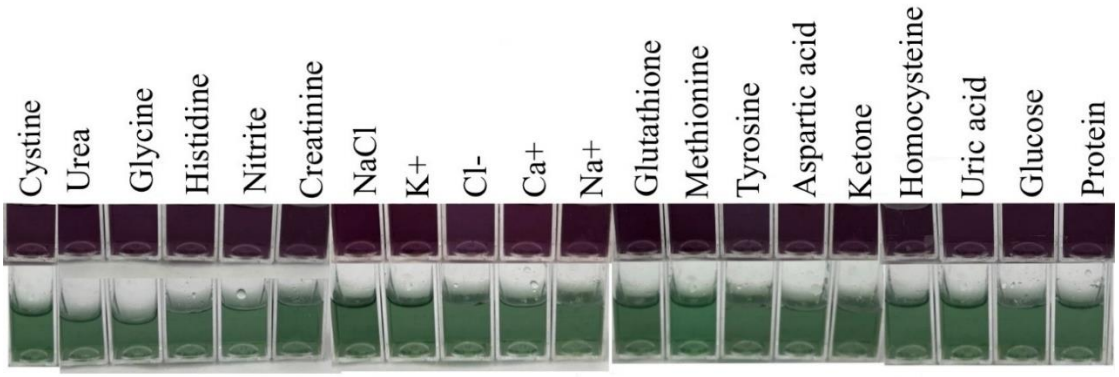

Fig. 19 - Interference study

To evaluate the selectivity of the Cr-DPC complex toward cysteine, an interference study was conducted using common urinary analytes at their physiological concentrations. Analytes such as urea, glycine, histidine, nitrite, creatinine, NaCl, K^+, Cl^-, Ca^{2+}, Na^+, glutathione, methionine, tyrosine, aspartic acid, ketone bodies, homocysteine, uric acid, glucose, protein, and ascorbic acid were tested.

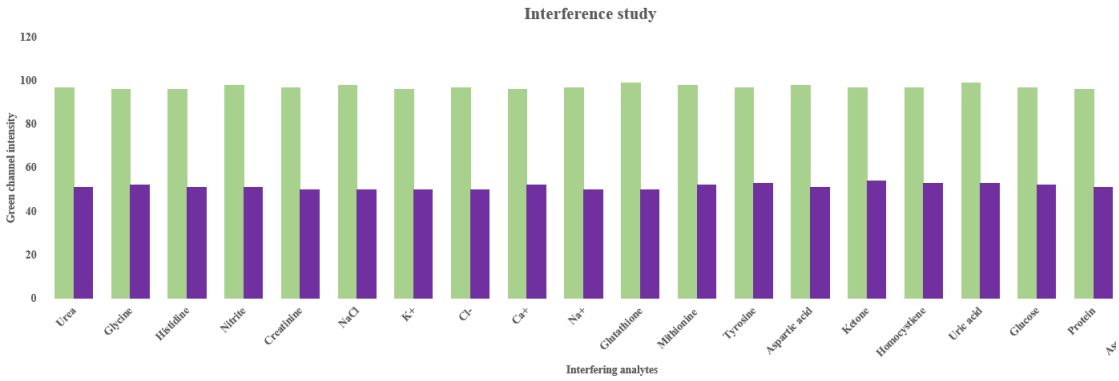

Fig. 20. RGB Analysis of inference study

The results showed no significant colour change or interaction between the Cr-DPC complex and any interfering species, with all samples retaining the purple colour of the complex. Only cysteine (500 µg/mL) triggered a distinct colour change from purple to green, indicating specific binding.

RGB analysis further confirmed that only cysteine increased the green channel intensity, while other analytes had no effect. This demonstrates the complex's high selectivity and strong anti-interference capability for cysteine detection in biological samples.

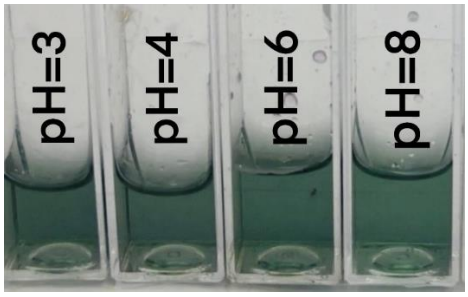

Fig. 21. Interference study of pH

Similarly, to assess the effect of pH variation on the complex's selectivity, interference studies were performed across pH 3 to pH 8, simulating possible urine pH ranges. The pH was adjusted using buffer solutions. The Cr-DPC complex maintained its colorimetric response, showing a consistent color change from purple to green in the presence of cysteine (500 µg/mL) at all tested pH levels. This confirms the stability and reliability of the detection system under varying physiological pH conditions.

4.7.Time-dependent study of colorimetric reaction

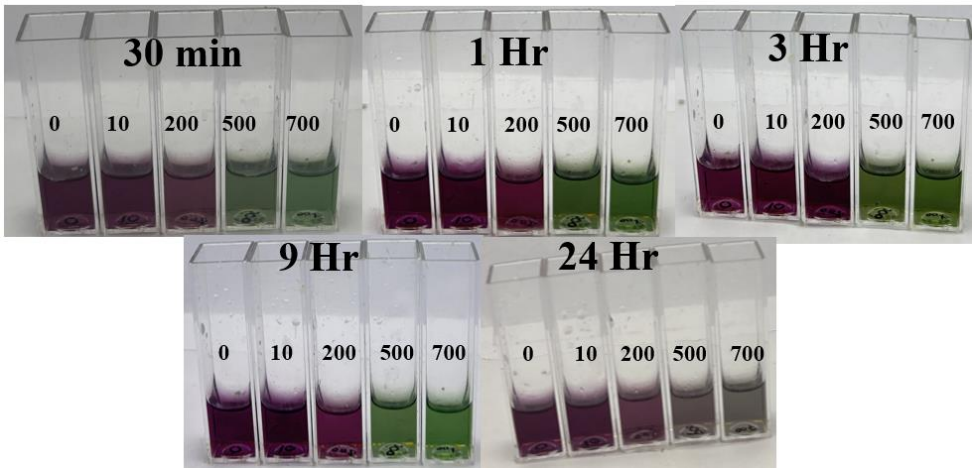

Fig. 22. Gradient obtained at different time stamp

A time-dependent study was conducted to evaluate the colour stability of the Cr-DPC complex with cysteine. The colour change from purple to green appeared clearly within 30 minutes, correlating with the cysteine concentration, and was easily visible to the naked eye. This indicates that the reaction completes within 30 minutes, making it suitable for rapid visual detection. Further observation at 1, 3, and 9 hours showed gradual brightening of the green colour, likely due to slow stabilization or rearrangement of the complex. However, a slight decrease in intensity was observed at 24 hours, possibly due to gradual degradation, oxidation, or precipitation of the complex. External factors like light exposure or evaporation might also contribute to this decline. Overall, the system provides quick detection within 30 minutes and remains stable for several hours, with maximum colour intensity around 9 hours.

4.8. Read out method

4.8.1. Arduino Mega 2560. Microcontroller Platform

The Arduino Mega 2560 is a robust, open-source development board that is built around the Atmel ATmega2560 8-bit microcontroller[29]. It boasts 54 digital I/O pins, including 15 that are capable of PWM, 16 analog input channels, and 4 hardware serial communication ports (UARTs), making it particularly well-suited for data collection and control in multisensor applications. With 256 KB of flash memory, 8 KB of SRAM, and 4 KB of EEPROM, it offers ample storage and processing capability for intricate sensing algorithms, real-time operations, and data storage[30]. In this project, the Mega 2560 is utilized as the primary processing and control unit to interface with the TCS230 color sensor, regulate timing functions for signal acquisition[31], and send the processed RGB and HSV values to a PC interface for analysis in real-time. Its standard 5V logic level and wide array of pins

enable direct connection with the TCS230 module without requiring any logic level shifting.

Fig. 23. - Arduino mega2560

4.8.2. TCS230 Color Sensor. Optical Measurement System

The TCS230 (also referred to as TCS3200 in various models) is a programmable device that converts color to frequency[32], incorporating a photodiode array, a current-to-frequency converter, and digital control circuitry all within a single integrated unit. It features an 8×8 grid of photodiodes[33] that are specifically filtered to detect red, green, blue, or clear light (unfiltered). The internal multiplexing system permits the selection of one-color channel at a time, facilitating the analysis of discrete RGB components. The photodiodes produce a current in relation to the intensity of the incoming light, which is then transformed into a square wave that has a frequency directly proportional to the intensity of the light[34]. This frequency output can be conveniently read using the digital input pins of an Arduino.

To maintain precision and repeatability in colorimetric assessments, the sensor is housed within a specially designed light-isolated chamber, which is lined with matte white reflective paper to reduce extraneous light and color distortion. Lighting is supplied by a constant-intensity white LED ring, along with light diffuser sheet, ensuring that illumination remains uniform during measurements. A cuvette holder positions the liquid sample

at a right angle to the sensor in order to enhance spectral reflectance and transmission properties.

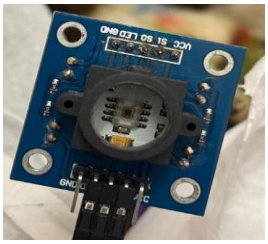

Fig. 24. - TCS230 Camera sensor

4.8.3. System Integration and Workflow

The TCS230 sensor interfaces with the Arduino Mega 2560 using four digital I/O pins.

- S0 and S1. Selection for frequency scaling
- S2 and S3. Selection for color filter (R/G/B)

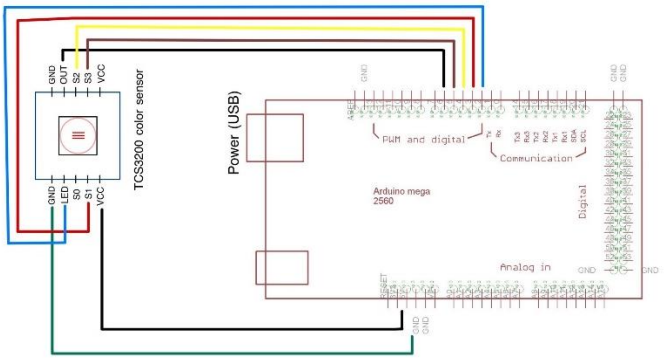

Fig. 25. Circuit schematic

OUT. Frequency output signal sent to Arduino (measured using pulseIn)

A microcontroller routine systematically selects each color filter using S2 and S3, retrieves the frequency for each filtered color with the pulseIn() function, and calculates the corresponding RGB values. These raw values

are then normalized and transformed into the HSV (Hue, Saturation, Value) color model to better align with human color perception and to enhance interpretability in biochemical contexts.

The acquired data is transmitted to a computer interface through USB serial communication, enabling real-time logging and optional visualization of the data. This conFig.uration allows for semi-automated colorimetric detection applicable to analytical tasks such as quantifying cysteine, where changes in color due to analyte interactions with chromogenic reagents correlate to measurable RGB/HSV values.

4.8.4. Objective-Specific Implementation

The main goal of this instrumentation system is to deliver a budget-friendly, dependable, and real-time method for assessing colorimetric variations in liquid samples for biosensing or chemical assay purposes. By utilizing the programmable capabilities of the Arduino Mega 2560 along with the spectral sensitivity of the TCS230, the system facilitates.

- High-precision detection of changes in RGB intensity[35]
- Consistent and calibrated color sensing within a controlled optical setting[36]

In the context of cysteine detection through a chromophore-based colorimetric assay, this system enables accurate quantification of gradual color transitions in the red-blue spectrum across a broad concentration range. The digital output nature of the TCS230 effectively minimizes analog noise[37], while the Arduino's robust I/O management provides adaptable integration for additional sensors or actuated control mechanisms.

4.8.5. Comparison of RGB values obtained by color grab app and Arduino read-out

To validate the performance of the developed device, the RGB values obtained from the TCS230 color sensor were compared with those acquired

using the Color Grab mobile application. As shown in the Fig.ure, both systems exhibited a strong linear correlation between green channel intensity and cysteine concentration spiked in real urine samples, with R^2 values of 0.97 for the Color Grab app and 0.96 for the device. The similarity in slope and intercept values, confirms the device's accuracy and reliability in detecting subtle color changes. This close agreement validates the practical applicability of the device as a low-cost alternative for quantitative colorimetric analysis.

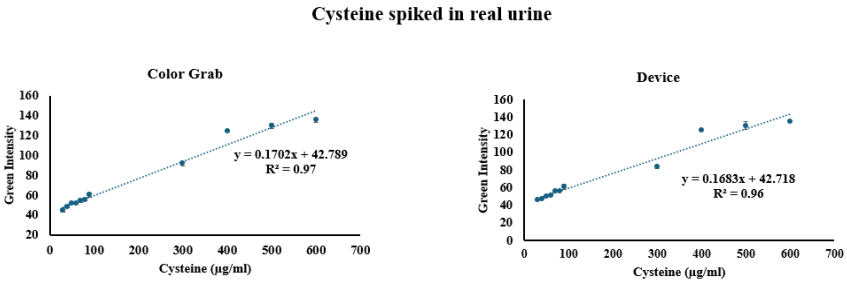

Fig. 26. - RGB values obtained by Color grab app and device

Chapter 5

Conclusion and Scope for Future Work

This study presents a multidisciplinary approach to the development of a portable, cost-effective colorimetric sensing system for the quantitative and visual detection of analyte concentration, with a focus on cysteine detection using a Chromium(III)-diphenylcarbazone (Cr-DPC) complex. The system integrates analytical chemistry, embedded electronics, and colorimetric image processing through the combined use of an Arduino Mega 2560 microcontroller and a TCS230 color sensor.

Chemically, the sensing mechanism is based on the formation of a Cr-DPC complex that undergoes a distinctive color transformation upon interaction with cysteine. The color change—from deep purple to green—is both rapid and concentration-dependent, occurring within 30 minutes of cysteine addition. This reaction was shown to be highly selective, with no observable interference from other urinary constituents, and stable up to 9 hours, with only minor fading after 24 hours. Such properties establish the assay's suitability for short- to intermediate-term detection in physiological environments, especially within the pH range typical of human urine.

In this context, the Arduino-based device serves as a practical platform for quantitative monitoring of the colorimetric change. The TCS230 sensor measures raw RGB values from the solution contained in a cuvette under standardized illumination conditions. These values are then converted to HSV color space, where the hue (H) component correlates more linearly and robustly with the concentration of cysteine, compared to raw RGB. The HSV space effectively decouples chromatic information from brightness and saturation, making it less sensitive to environmental lighting and sensor noise. For enhanced user feedback, the processed HSV values are optionally converted back to normalized RGB for digital visualization or display output, thus combining analytical precision with human readability.

The system successfully mapped a smooth and interpretable color gradient ranging from purple (0 µg/mL) to brownish-yellow (90–300 µg/mL), and finally green (400–600 µg/mL), mirroring the chemical transformation induced by cysteine concentration. The real-time nature of this detection process, alongside the portability and affordability of the hardware, makes the system highly promising for point-of-care diagnostics. In particular, it provides a viable tool for non-invasive monitoring of cysteine levels in patients with cystinuria, supporting early detection and ongoing disease management.

In conclusion, this work demonstrates that the integration of simple yet effective chemistry with open-source electronics and colorimetric processing algorithms can yield an accurate, stable, and accessible biosensing device. Future directions may include integrating wireless data transmission, app-based tracking, and adaptation to multiplexed detection of other biologically relevant analytes.

REFERENCES

1. The colorimetric and microfluidic paper-based detection of cysteine and homocysteine using 1,5-diphenylcarbazide-capped silver nanoparticles - RSC Advances (RSC Publishing) DOI:10.1039/D0RA08615K. https://pubs.rsc.org/en/content/articlehtml/2021/ra/d0ra08615k.
2. Multicolor emission-based nitrogen, sulfur and boron co-doped photoluminescent carbon dots for sequential sensing of Fe3+ and cysteine: RGB color sensor and live cell imaging - ScienceDirect. https://www.sciencedirect.com/science/article/pii/S1386142523007254 .
3. Alawsi, T., Mattia, G. P., Al-Bawi, Z. & Beraldi, R. Smartphone-based colorimetric sensor application for measuring biochemical material concentration. *Sensing and Bio-Sensing Research* **32**, 100404 (2021).
4. XGBoost Model for Chronic Kidney Disease Diagnosis | IEEE Journals & Magazine | IEEE Xplore. https://ieeexplore.ieee.org/abstract/document/8693581.
5. Cruz-Rojas, T., Franco, J. A., Hernandez-Escobedo, Q., Ruiz-Robles, D. & Juarez-Lopez, J. M. A novel comparison of image semantic segmentation techniques for detecting dust in photovoltaic panels using machine learning and deep learning. *Renewable Energy* **217**, 119126 (2023).
6. Frontiers | Point-of-care system for rapid real-time detection of SARS-CoV-2 virus based on commercially available Arduino platforms. https://www.frontiersin.org/journals/bioengineering-and-biotechnology/articles/10.3389/fbioe.2022.917573/full.
7. D'Ambrosio, V., Capolongo, G., Goldfarb, D., Gambaro, G. & Ferraro, P. M. Cystinuria: an update on pathophysiology, genetics, and clinical management. *Pediatr Nephrol* **37**, 1705–1711 (2022).
8. Trinchieri, A., Dormia, G., Montanari, E. & Zanetti, G. Cystinuria: definition, epidemiology and clinical aspects. *Arch Ital Urol Androl* **76**, 129–134 (2004).

9. Suryati, L., Sulistyarti, H. & Atikah, A. Development of Spectrophotometric Method for Determination of Chromium Species Using Hypochlorite Agent Based on the Formation of Cr(VI)-Diphenylcarbazide Complex. *The Journal of Pure and Applied Chemistry Research* **4**, 34–41 (2015).
10. Cysteine Metabolism in Neuronal Redox Homeostasis: Trends in Pharmacological Sciences. https://www.cell.com/trends/pharmacological-sciences/abstract/S0165-6147(18)30045-2.
11. Doi, R. Red-and-green-based pseudo-RGB color models for the comparison of digital images acquired under different brightness levels. *Journal of Modern Optics* **61**, 1373–1380 (2014).
12. A Background Modeling and Foreground Detection Algorithm Using Scaling Coefficients Defined With a Color Model Called Lightness-Red-Green-Blue | IEEE Journals & Magazine | IEEE Xplore. https://ieeexplore.ieee.org/abstract/document/8118166.
13. Phys. Rev. E 69, 037105 (2004) - Red-green-blue model. https://journals.aps.org/pre/abstract/10.1103/PhysRevE.69.037105.
14. Dual-color GRAB sensors for monitoring spatiotemporal serotonin release in vivo | bioRxiv. https://www.biorxiv.org/content/10.1101/2023.05.27.542566v1.abstract.
15. Learning a Contact Potential Field for Modeling the Hand-Object Interaction | IEEE Journals & Magazine | IEEE Xplore. https://ieeexplore.ieee.org/abstract/document/10478277.
16. Claes, D. J. & Jackson, E. Cystinuria: mechanisms and management. *Pediatr Nephrol* **27**, 2031–2038 (2012).
17. Biyani, C. S. & Cartledge, J. J. Cystinuria—Diagnosis and Management. *EAU-EBU Update Series* **4**, 175–183 (2006).
18. Cystinuria: an inborn cause of urolithiasis | Orphanet Journal of Rare Diseases. https://link.springer.com/article/10.1186/1750-1172-7-19.

19. NOVEL RENAL AMINO ACID TRANSPORTERS | Annual Reviews. https://www.annualreviews.org/content/journals/10.1146/annurev.physiol.67.031103.153949.
20. Metabolic consequences of cystinuria | BMC Nephrology. https://link.springer.com/article/10.1186/s12882-019-1417-8.
21. Challacombe, B. & Bultitude, M. F. The kidneys, urinary tract and prostate. in *Browse's Introduction to the Symptoms & Signs of Surgical Disease* (CRC Press, 2021).
22. Clinical assessments and care interventions to promote oral hydration amongst older patients: a narrative systematic review | BMC Nursing. https://link.springer.com/article/10.1186/s12912-016-0195-x.
23. Update on cystine stones: current and future concepts in treatment. https://www.jstage.jst.go.jp/article/irdr/9/2/9_2020.03006/_article/-char/ja/.
24. Fully automated assay for total homocysteine, cysteine, cysteinylglycine, glutathione, cysteamine, and 2-mercaptopropionylglycine in plasma and urine | Clinical Chemistry | Oxford Academic. https://academic.oup.com/clinchem/article-abstract/44/4/825/5642620.
25. Highly selective optical and naked-eye recognition of L-cystine through spectroscopy and development of cellulose paper nano biosensor test strips for the early diagnosis of cystinuria - ScienceDirect. https://www.sciencedirect.com/science/article/pii/S0026265X24015911.
26. Sadiq, S. & Cil, O. Cystinuria: An Overview of Diagnosis and Medical Management. *Turk Arch Pediatr* **57**, 377–384 (2022).
27. Leslie, S. W., Sajjad, H. & Nazzal, L. Cystinuria. in *StatPearls* (StatPearls Publishing, Treasure Island (FL), 2024).
28. Servais, A. *et al.* Cystinuria: clinical practice recommendation. *Kidney International* **99**, 48–58 (2021).

29. Barrett, S. F. Arduino Platforms. in *Arduino I: Getting Started* (ed. Barrett, S. F.) 33–73 (Springer International Publishing, Cham, 2020). doi:10.1007/978-3-031-79915-0_2.
30. Yayavaram, N., Rajan, S. & Vardhan, V. ARM Processor Based Multisensor System Design for the Measurement of Environmental Parameters. *Sensors and Transducers* **136**, 59–71 (2012).
31. A New Technique for Improving the Estimation of a Reflective Optical Color Sensor | Sensing and Imaging. https://link.springer.com/article/10.1007/s11220-020-0276-5.
32. Huang, L. *et al.* A portable dual-mode colorimetric and fluorescence sensing platform for RGB detection in liquid solutions. *Measurement* **242**, 116091 (2025).
33. Kumar, S., Mishra, P. & Islam, T. Condition Monitoring of Transformer Breather Using Smart Photodiodes Array. *IEEE Transactions on Instrumentation and Measurement* **73**, 1–7 (2024).
34. Ghorude, T., Chaudhari, A. & Shaligram, A. Quantitative color measurement of pH indicator paper using Trichromatic LEDs and TCS230 color sensor. *Proc SPIE* **7375**, (2008).
35. I., M. R. & Avalos-Gonzalez, D. Precision and Versatility in Color Sensing: A Comprehensive Characterization of the TCS3200 Using Time Domain Analysis. in *2024 International Conference on Electrical, Computer and Energy Technologies (ICECET* 1–6 (2024). doi:10.1109/ICECET61485.2024.10698668.
36. El-Hageen, H. M. M. A New Technique for Improving the Estimation of a Reflective Optical Color Sensor. *Sens Imaging* **21**, 12 (2020).
37. A Case Study on Assistive Technology for Visual Impairment Individuals: Adaptations in Household Appliances | Journal of Control, Automation and Electrical Systems. https://link.springer.com/article/10.1007/s40313-013-0100-8.